A quantitative magnetic braking experiment

Cyrus S. MacLatchy, Philip Backman, and Larry Bogan

Citation: Am. J. Phys. **61**, 1096 (1993); doi: 10.1119/1.17356
View online: http://dx.doi.org/10.1119/1.17356
View Table of Contents: http://ajp.aapt.org/resource/1/AJPIAS/v61/i12
Published by the American Association of Physics Teachers

Related Articles

A demonstration condenser microphone
Phys. Teach. 50, 508 (2012)

Dashboard Videos
Phys. Teach. 50, 477 (2012)

Peer Assessment with Online Tools to Improve Student Modeling
Phys. Teach. 50, 489 (2012)

Analyzing spring pendulum phenomena with a smart-phone acceleration sensor
Phys. Teach. 50, 504 (2012)

Locating the Center of Gravity: The Dance of Normal and Frictional Forces
Phys. Teach. 50, 456 (2012)

Additional information on Am. J. Phys.

Journal Homepage: http://ajp.aapt.org/

Journal Information: http://ajp.aapt.org/about/about_the_journal

Top downloads: http://ajp.aapt.org/most_downloaded

Information for Authors: http://ajp.dickinson.edu/Contributors/contGenInfo.html

ADVERTISEMENT

$$T(z)=\frac{1}{c}\int_0^{\sqrt{a^2-z^2}} 2\pi\rho\, d\rho \frac{j(\sqrt{\rho^2+z^2})}{\sqrt{\rho^2+z^2}}=\int_z^a 2\pi\frac{1}{c}j(r)dr \tag{C10}$$

and so

$$\frac{2\pi}{c}j(\rho)=-\frac{d}{d\rho}T(\rho)=-\frac{d}{d\rho}\int_{-\sqrt{a^2-\rho^2}}^{\sqrt{a^2-\rho^2}}\frac{\lambda(\sqrt{x^2+\rho^2})dx}{\sqrt{x^2+\rho^2}}. \tag{C11}$$

[1]See Ref. 2 and references therein and in Eyges, Ref. 4.

[2]E. W. Hobson, "On Green's function for a circular disc, with application to electrostatic problems," Trans. Cambridge Philos. Soc. **18**, 277–291 (1900).

[3]L. C. Davis and J. R. Reitz, "Solution to potential problems near a conducting semi-infinite sheet or conducting disc," Am. J. Phys. **39**, 1255–1265 (1971).

[4]E. T. Copson, "On the problem of the electrified disc," Proc. Edinburgh Math. Soc. **8**, 14–19 (1947). See also Leonard Eyges, *The Classical Electromagnetic Field* (Dover, New York, 1980), p. 68.

[5]L. C. Davis, E. M. Logothetis, and R. E. Soltis, "Stability of magnets levitated above superconductors," J. Appl. Phys. **64**, 4212–4218 (1988).

[6]W. Saslow, "How a superconductor supports a magnet, how magnetically 'soft' iron attracts a magnet, and eddy currents for the uninitiated," Am. J. Phys. **59**, 16–25 (1991).

[7]W. Smythe, *Static and Dynamic Electricity* (McGraw-Hill, New York, 1968), pp. 91–92.

[8]Landau and Lifschitz, *Electrodynamics in a Continuous Medium* (Pergamon, London, 1960), Chap. 1, Paragraph 3.

[9]J. D. Jackson, *Classical Electrodynamics* (Wiley, New York, 1962), Sec. 9.7.

[10]The reader may demonstrate this explicitly by introducing Cartesian coordinates rotated by ϕ_0. On the chord of Fig. 1(b), these coordinates are equal to $(\tilde{x}=\rho_0, \tilde{y}=\rho_0\tan\theta)$, where $\theta=\phi'-\phi_0$. The ds in Eq. (6) can be replaced by $d\tilde{y}$, and the factor $\cos m\phi'$ expressed in terms of ϕ_0 and θ. The term in $\sin m\theta$ vanishes on integration.

A quantitative magnetic braking experiment

Cyrus S. MacLatchy, Philip Backman, and Larry Bogan
Department of Physics, Acadia University, Wolfville, Nova Scotia, B0P 1X0, Canada

(Received 29 September 1992; accepted 1 April 1993)

A popular demonstration which often accompanies the introduction of magnetic induction is that in which a strong button-shaped magnet is dropped through a long copper or aluminum tube. The induced currents cause a retarding force which dramatically slows the descent of the falling magnet. Here, we describe methods of calculating and measuring the terminal velocity and magnetic forces in the magnetic braking experiment. The techniques are quite accurate, inexpensive to perform, and are suitable for introductory courses in electricity and magnetism.

I. INTRODUCTION

A popular demonstration often used in introductory physics courses to illustrate the effects of magnetic induction is the one in which a strong button magnet is dropped through a vertical copper or aluminum pipe. The changing magnetic flux caused by the falling magnet induces eddy currents in the pipe and the resulting forces cause the magnet to fall with a much reduced velocity. Students observing the demonstration for the first time expect the magnet to descend at its freefall velocity and their response is often accompanied by exclamations of surprise. Our experiment is based on this popular demonstration. To make the experiment quantitative, we wrap a magnetic pickup coil around the copper pipe and take a little more care in setting up the experiment than one normally does in the lecture room demonstration.

Other experiments involving the braking action of a magnetic field have been analyzed elsewhere. In their article, Wiederick *et al.*[1] have presented a simple theory of magnetic braking in a thin metal strip and have used it to test the retarding action on a spinning aluminum disk. An alternative analysis of the same experiment is presented by Heald.[2] Marcuso *et al.*[3,4] have considered the braking effect of a localized magnetic field on a spinning disk. They present both a careful calculation of the localized nonuniform field from a small magnet[3] and an experimental analysis of the deceleration of a spinning disk[4] based on these calculations. Rossing and Hull[5] have written a fairly extensive review article on magnetic levitation which involves principles identical to those encountered in the analysis of braking experiments. More recently, Saslow[6] has made a comprehensive study of Maxwell's theory of eddy currents in thin conducting sheets and has applied these concepts to MAGLEV transportation systems. Saslow also discusses the magnetic braking experiment which is the subject of this paper. By assuming that the magnetic field of the falling magnet can be approximated by a dipole, he has been able to calculate the terminal velocity of the falling magnet. As will be seen later, this calculation overestimates the velocity.

An advantage of the present system is its simple geometry. As the button magnet falls through the vertical pipe, its axis is aligned with that of the pipe. This forces axial symmetry on the interaction between the magnetic field and the cylindrical conducting wall and consequently produces a geometry in which the currents and forces have cylindrical symmetry. By applying the basic laws of electricity and magnetism, we have been able to relate the

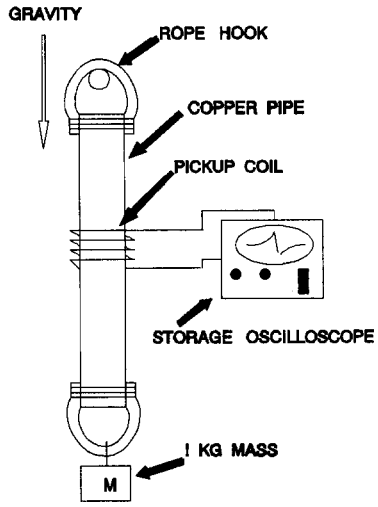

Fig. 1. The apparatus consists of a suspended copper pipe and an embedded pickup coil which is connected to a digital oscilloscope.

Table I. Pertinent experimental parameters.

Button magnet (neodymium)	
Length	6.4 mm
Length (with tape)	$\approx$18 mm
Diameter	12.6 mm
Magnetic moment	0.67 A m^2
Weight (with tape)	0.060 N
Copper pipe	
Inside radius	7.29 mm
Outside radius	7.96 mm
Conductivity	5.08×10^7 Ω^{-1} m^{-1}
Wall thickness (δ)	0.67 mm
Center of wall (R)	7.625 mm
Pickup coil	
Wire diameter	0.275 mm
Number of turns	9
Terminal velocity of falling magnet	
Measured	12.7 ± 0.4 cm s^{-1}
Dipole model	17.8 cm s^{-1}
Numerical model	13.0 cm s^{-1}

weight of the magnet and hence, the magnetic force, to the induced electromagnetic force (EMF). Although we use a digital oscilloscope to display the electrical signal, the experiment could be interfaced to a digital computer through an inexpensive A/D conversion board. In first year labs, the slow speed at which the magnet falls is a nice feature of the experiment, since it allows the student to see the evolution of the trace on the oscilloscope as the magnet passes through the pickup coil. There is an immediate and obvious connection between the oscilloscope trace and the eddy currents circulating in the copper pipe.

In our presentation, we carry through two calculations. In the first, the electrical power being dissipated in the copper pipe is equated to the gravitational work being done on the magnet as it falls. This enables us to measure the weight of the magnet "electrically." Although we talk about the weight here, we are actually measuring the magnetic force on the falling magnet, since at equilibrium, when the magnet is falling at terminal velocity, these two forces, the gravitational and magnetic, have the same magnitude. In the second calculation, we measure the strength of the magnetic field of the magnet with a gaussmeter. This enables us to determine the dipole moment of the magnet which is then used in a numerical calculation to evaluate the radial magnetic field in the copper pipe. Knowing the radial magnetic field in the pipe enables us to predict either the terminal velocity or the magnetic force on the magnet. The values calculated from the theory and the experimental measurements are in good agreement, a feature which is always welcomed by the student. The time required for the measurements is relatively short and the cost of the apparatus is likely to be less than $100 if standard measuring equipment such as an oscilloscope, a computer, and/or a gaussmeter are available.

II. THE EXPERIMENT

The apparatus is shown in Fig. 1. It consists of a suspended copper pipe, about 0.5 m in length, with an embedded pickup coil (9 turns) connected to a digital oscilloscope. The pickup coil is made from fine, varnished magnet wire. The coil lead wires are twisted to minimize extraneous magnetic pickup from the falling magnet and other

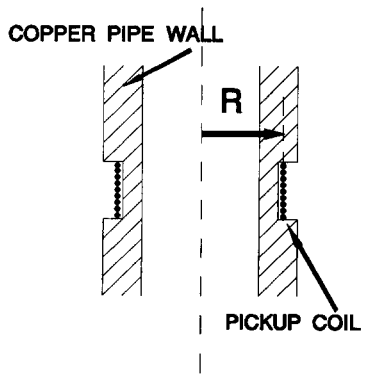

Fig. 2. The pickup coil is embedded in the wall of the copper pipe at a radius R.

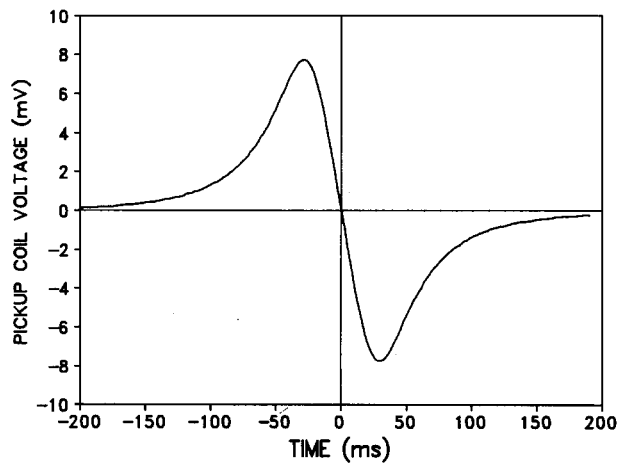

Fig. 3. As the button magnet passes through the pickup coil, it generates a trace on the oscilloscope. The wave form shown here is for a 9-turn pickup coil.

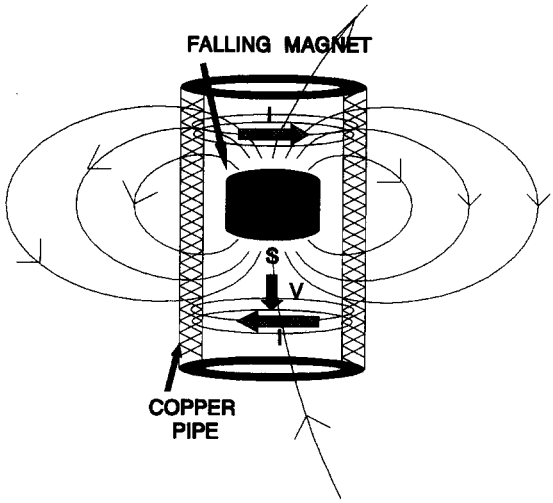

Fig. 4. As the button magnet falls through the pipe, it generates eddy currents (I) which interact with the magnetic field and impede the rate of fall. The horizontal arrows show the direction of the current. Here, the south pole of the magnet (S) and the terminal velocity (V) point down.

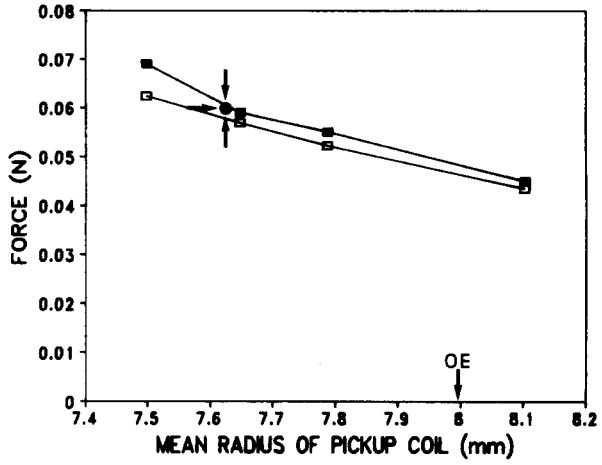

Fig. 5. The magnetic force on the magnet is plotted as a function of the embedded radius of the pickup coil. One curve is generated from the signal observed on the oscilloscope (■) while the other is based on the computed value of B_r (□). The highlighted point represents the measured weight of the magnet plotted at the center of the pipe wall. The outer edge (OE) of the pipe is also indicated on the figure.

influences of electrical noise in the lab environment. As shown in Fig. 2, the coil would normally be embedded in the copper pipe to make sure that the coil wire lies at the center of the conducting wall. In our experiment, we placed the coil at a variety of depths to test our understanding of the theory. The suspension from the top ensures that the pipe hangs vertically.

We used inexpensive, 1/2-in. copper pipe, available in 12-ft lengths from a local building supply outlet. Since we were not certain of its composition and resistivity, we borrowed 10, 12-ft lengths from our supplier and measured the resistance of the copper pipe as a function of its length. We did this by measuring the resistance of the pipe with a sensitive 4-wire ohmmeter as we shorted out sections of the pipe which were connected in series by short lengths of very tightly clamped copper braid. The resistivity was computed from the slope of the resistance vs length graph and the dimensions of the pipe. Its value is listed in Table I along with the dimensions of the pipe.

For our magnet, we used a small, cylindrical neodymium[7] magnet having a diameter of 12.6 mm and a length of 6.4 mm. A single layer of transparent office tape was wrapped around the magnet to make of it a longer cylindrical shape of about 18 mm length. This procedure improves the magnet's stability as it falls through the pipe and reduces its tendency to wobble. Care must be exercised to avoid letting these magnets fall on any hard surface as they are quite brittle. Since it falls quite slowly, we generally caught the magnet with our hands as it fell out of the pipe. A Hall effect gaussmeter was used to measure the strength of the magnetic field at several positions on the symmetry axis of the magnet. These values are used to determine the magnetic moment which is used in a computer model to predict the radial field. It is also necessary to weigh the magnet. The dimensions, magnetic moment, and weight of the magnet appear in Table I.

In a typical experiment, the neodymium magnet is dropped down the center of the pipe and induces a voltage in the coil which is recorded on the oscilloscope. A typical trace of the EMF as a function of time is shown in Fig. 3. In the following section, we shall show how this data can be used to measure the magnetic force on the magnet.

III. POWER DISSIPATION AND GRAVITATIONAL ENERGY

As the button magnet falls through the pipe, the changing magnetic flux generates eddy currents which flow in the θ or azimuthal direction. The magnet quickly reaches terminal velocity and the currents reach a steady state value. The magnitude of the eddy current at any position is related to the changing flux by Faraday's Law. The diagram in Fig. 4 represents the magnet, its field, and the eddy currents in the wall of the copper tube. Two current lobes flowing in opposite directions are formed, one above and one below the falling magnet. For our magnet and pipe, a total current of about 5 A flows in each lobe.

In this derivation, we are going to relate the weight of the falling magnet to the electromotive force detected by the pickup coil and the properties of the pipe. For a magnet falling at constant velocity, the electrical power dissipated in the pipe is equal to the rate at which gravitational energy is lost by the magnet. The power dissipated in a volume element dV is

$$dP=\mathbf{J}\cdot\mathbf{E}\,dV, \tag{1}$$

where $\mathbf{J}$ is the current density and $\mathbf{E}$ is the electric field. For the cylindrical geometry of our problem, it is convenient to rewrite this equation as

$$dP=J_\theta(r,z)E_\theta(r,z)2\pi r\,dr\,dz, \tag{2}$$

where it has been assumed that the θ components of $\mathbf{J}$ and $\mathbf{E}$ are functions of r and z. Now J_θ can be eliminated by noting that $\mathbf{J}=\sigma\mathbf{E}$ where σ is the electrical conductivity of the pipe. For a thin walled pipe, we replace dr with δ, the thickness of the wall, and assume that E_θ is an average value measured in the middle of the pipe wall at a radial distance R from the axis. The power dissipated in the element of length dz is thus

$$dP=\sigma E_\theta^2(z)2\pi R\delta\, dz. \tag{3}$$

The average electric field in the copper pipe is related to the EMF, ϵ, detected by the coil at position z, by the following equation,

$$E_\theta(z)=\frac{\epsilon}{2\pi R}. \tag{4}$$

The voltage measured on the oscilloscope is related to ϵ by $V(t)=N\epsilon(t)$ where N is the number of turns in the coil. The coil voltage is time dependent but can be related to the z coordinate by noting that $dz=vdt$ where v is the terminal velocity of the falling magnet. Finally, the total electrical power is found by substituting Eq. (4) into Eq. (3) and integrating. Thus

$$P=\frac{v\sigma\delta}{2\pi R}\int_{t_1}^{t_2}\epsilon^2\, dt, \tag{5}$$

where t_1 and t_2 are chosen so as to include the entire wave form generated by the pickup coil. Now the rate at which gravitational work is being done on the falling magnet is mgv. Thus the weight of the magnet and the magnetic force, since they are of equal magnitude when the magnet is falling at the terminal velocity, are related to the coil signal by

$$F_M=mg=\frac{\sigma\delta}{2\pi R}\int_{t_1}^{t_2}\epsilon^2\, dt=\frac{\sigma\delta}{2\pi RN^2}\int_{t_1}^{t_2}V^2(t)dt. \tag{6}$$

The voltage $V(t)$ is normally measured at the mean radius, R. To determine the sensitivity to the positioning of the pickup coil, we calculated the magnetic force by evaluating the right-hand side of Eq. (6) for several positions of the coil winding: first, on the outside surface of the pipe and then at several different groove depths. A plot of these values as a function of the coil's distance from the axis of the pipe is shown in Fig. 5. Notice that Eq. (6) gives the correct weight when the center of the coil is placed near the center of the pipe wall.

It is worthwhile noting that Eq. (6) has been derived without the use of concepts beyond Faraday's law and the integration was performed on a microcomputer with the aid of a short BASIC program. Thus this experiment could be performed at the introductory physics level.

IV. VELOCITY OF THE FALLING MAGNET

The velocity of the falling magnet can be predicted by considering the retarding force acting on the magnet or, conversely, on the current circulating in the pipe. In a manner similar to that used by Marcuso *et al.*,[3] the current density can be represented as $\mathbf{J}=\sigma\mathbf{E}=\sigma(\mathbf{v}\times\mathbf{B})$ and we can write $J=\sigma E_\theta=\sigma vB_r$ for the present geometry. Thus, the eddy current circulating in a ring-shaped element of the pipe having height dz is just

$$J\delta\, dz=\sigma E_\theta\delta\, dz=\sigma vB_r\delta\, dz. \tag{7}$$

In Eq. (7), $J\delta$ has the dimensions of current per unit length. The force on a segment of the ring is given by

$$\mathbf{dF}=J\delta\mathbf{dl}\times\mathbf{B}\, dz, \tag{8}$$

where $\mathbf{dl}$ is an element of length taken in the θ direction. This element of force has components which point in both the radial and axial directions. If we integrate around the circumference of the ring, the radial component of the force disappears and we are left with a z component

$$dF_z=2\pi RJ\delta B_r\, dz=2\pi R\sigma v\delta B_r^2\, dz. \tag{9}$$

The total force acting on the magnet is obtained by integrating Eq. (9). By rearranging and setting the total force equal to the weight of the magnet we get the terminal velocity

$$v=\frac{mg}{2\pi R\sigma\delta\int_{z_1}^{z_2}B_r^2\, dz}. \tag{10}$$

This equation represents the terminal velocity of the falling magnet in terms of the weight of the magnet, the dimensions of the pipe, the conductivity of the pipe, and the magnetic field of the magnet. Several of these parameters can be eliminated by replacing the weight of the magnet with its value from Eq. (6). If this is done, we find that

$$v=\frac{\int_{t_1}^{t_2}V^2(t)dt}{(2\pi R)^2N^2\int_{z_1}^{z_2}B_r^2\, dz}. \tag{11}$$

This equation can be used to calculate v without the need of determining a value for σ. However, Eq. (11) does not explicitly represent the terminal velocity in terms of the basic properties of the apparatus, but represents a determination of the velocity of a falling magnet whether it be the terminal velocity or not. To evaluate either Eq. (10) or Eq. (11), B_r must be determined at the center of the pipe wall.

V. THE RADIAL MAGNETIC FIELD AND ITS INTEGRAL

Two methods of evaluating B_r were considered: one was based on measuring B_r directly and then using a polynomial to generate an integrable function, while the other was based on evaluating the dipole moment of the magnet and then calculating the value of B_r from a computer model. Although the direct measurement of B_r may seem the better choice, experimentally, it is the less accurate method because of the difficulty in precisely positioning the gaussmeter probe at off-axis positions. With the dipole technique, B_z is measured at several points on the axis of the magnet where the positioning is easier and the probe signal has a maximum when the probe is properly aligned with the field.

Let us begin by representing the field of the neodymium magnet by a dipole field.[8] Although this representation is inadequate near the magnet where the radius of the magnet is comparable to the distance from the center of the magnet to the field point, the dipole equations will be useful when the computer model is introduced later in the discussion. For a point on the axis of the magnet, the axial magnetic field is

$$B_z(z)=\frac{2\mu_0 m_B}{4\pi z^3} \tag{12}$$

and the radial magnetic field in the wall of the pipe at radius R is

$$B_r(z)=\frac{3\mu_0 m_B}{4\pi}\frac{Rz}{(R^2+z^2)^{5/2}}, \tag{13}$$

where m_B is the magnetic moment. If Eq. (13) is placed in Eq. (10) and integrated, an approximate value for the fall-

Table II. Axial magnetic field [$B_z(z)$ in tesla]. Distance in millimeters from the center of the magnet.

Distance	Measured	Dipole	Numerical
10	0.083 2	0.134	0.090 9
20	0.014 6	0.016 7	0.015 2
30	0.004 6	0.004 95	0.004 77
40	0.002 09	0.002 09	0.002 04
50	0.001 06	0.001 07	0.001 06

ing speed of the magnet can be obtained. The integral for the square of the magnetic field is

$$\int_{-\infty}^{+\infty} B_r^2\, dz = \frac{5\pi}{128}\frac{9\mu_0^2 m_B^2}{16\pi^2 R^5} \tag{14}$$

and the resulting velocity is

$$v = \frac{128(mg)(8R^4)}{45\sigma\delta\mu_0^2 m_B^2}. \tag{15}$$

This expression represents the dipole approximation for the terminal velocity and is identical to the expression published by Saslow.[6] For the magnet and copper pipe of our experiment, the value computed from Eq. (15) is about 40% larger than the measured value, both of which are recorded in Table I. In general, the accuracy of this equation will depend on the sizes of both the pipe and the magnet but it is mainly linked with the inability of the dipole model to correctly represent the magnetic field near the magnet.

A more accurate prediction of the radial magnetic field can be achieved with a numerical calculation of B_r. If we assume that the magnetization of the neodymium magnet is uniform throughout, then its external magnetic field is equivalent to that produced by a uniform electric current on its cylindrical surface. Thus, the magnet can be numerically simulated by a small coil of n turns, having the same dimensions and magnetic moment as the magnet. The relationship between the magnetic moment of such a coil and the current in its windings is

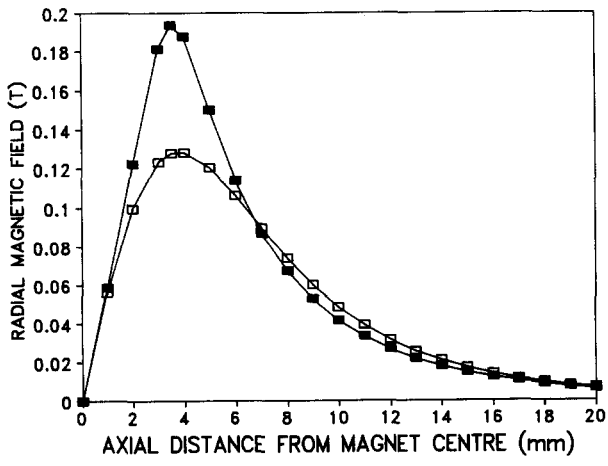

Fig. 6. The radial magnetic field computed from the dipole model (□) is less than that computed from the computer model (■) in the region near the magnet. The calculations are for $m_B = 0.67$ A m^2.

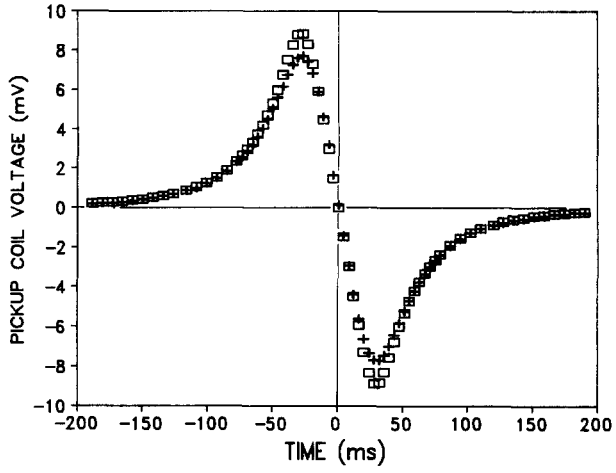

Fig. 7. These curves represent the EMF detected by the 9-turn pickup coil as the falling magnet passes through. One curve (+) is taken from the raw data on the oscilloscope screen while the other (□) is plotted from Eq. (17) as explained in the text.

$$m_B = \pi a^2 n I, \tag{16}$$

where a is the radius of the coil, here equal to that of the magnet. For our purposes, we chose n to be 15 although other values would be suitable. The computer model is similar to one developed by Merrill.[9] Each of the circular loops are divided into 36 straight segments and the Biot–Savart law is used to compute the components of the magnetic field at each point by summing the field produced by each of the segments. The final field of the coil is computed by summing the contributions from each of the 15 windings. The magnetic moment, and consequently the current in the windings, must be determined from measurements of the magnetic field.

To determine the magnetic moment, the axial magnetic field of the magnet was measured with a gaussmeter at distances of 10, 20, 30, 40, and 50 mm from the center of the magnet. The magnetic moment was determined by fitting Eq. (12) to the magnetic field values at 40 and 50 mm where the dipole best approximated the actual magnetic field. The resulting value for the magnetic moment was 0.67 A m^2. From Eq. (16), with $n=15$ and $a=6.3$ mm, the equivalent current flowing in the 15-turn coil of our model is 358 A, an interestingly large value for such a small coil. The measured axial magnetic field, the axial magnetic field computed from the dipole model, and the axial magnetic field computed from the coil model are compared in Table II. It is clear that the dipole model is less accurate near the magnet while the values generated by the computer model are closer to the measured field strength. The results of the modeling are shown in Fig. 6 where the strength of the radial magnetic field is shown for both the dipole and coil models. The field is for a magnetic moment of 0.67 A m^2 at a radius of 7.63 mm, the center of the pipe wall. As previously noted when the dipole field was used to compute the velocity of the falling magnet, the radial dipole field under estimates the field near the magnet.

VI. CALCULATIONS WITH B_r

When the results represented in Fig. 6 for the coil model are used to evaluate the integral in Eq. (10), the velocity of

the falling magnet is determined to be 13 cm s^{-1}. The velocity, determined by timing the magnet's fall through a 50-cm length of pipe with a stopwatch, is 12.7 ± 0.4 cm s^{-1}, in quite good agreement with the calculated value. We have attempted to compare the magnetic force with the viscous drag on the falling magnet to account for the lower value but find that the estimated drag forces are less than 0.1% of the magnetic force. Thus the terminal velocity quoted here is dominated by magnetic effects and the difference between the two measurements of velocity is most likely due to experimental error.

If we examine Eq. (7), we see that the pickup coil voltage can be related to the radial field. Thus

$$V(t) = N\epsilon(t) = N2\pi R E_\theta(t) = N2\pi R v B_r[z(t)], \quad (17)$$

where $z(t)$ represents the distance from the coil to the magnet at time t. If the data from Fig. 6 are used along with the velocity, then Eq. (17) can be used to generate the voltage wave form detected by the oscilloscope. This procedure has been followed to produce the theoretical curve seen in Fig. 7. Once again, the agreement between the measured EMF and the calculated value is quite good.

Finally, we use the predicted magnetic field and the terminal velocity to calculate the magnetic force and show the result in Fig. 5. The force computed from the EMF model [Eq. (6)] is also shown on the same figure. The values computed from the magnetic field are 3%–5% lower than those computed from the EMF model. Also shown on the graph is the measured weight of the magnet and the location of the center of the pipe wall. Notice that the two curves pass very close to this point, indicating that the best depth to place the pickup coil is at the center of the wall.

We have carried through several procedures to test the accuracy of our measurements and the computer modeling. For example, the accuracy of the computer model was tested by comparing its value for the axial magnetic field with that calculated from analytical equations for an identical coil. The difference was negligibly small. The uncertainty in the gaussmeter measurements were checked by calibrating the gaussmeter against the known field generated by a Helmholtz coil. The uncertainty was determined to be $\pm 3\%$.

A problem which we were unable to eliminate lies in the difficulty of determining an accurate value for the magnetic moment from the magnetic field measurements. As is easily seen in Eq. (12), the far axial field depends on $1/z^3$ so that any small error in the placement of the gaussmeter probe can generate a large error in the measured B_z. Since our experimental value of m_B is based on B_z, this error can have a serious effect on the measured value of m_B. As well, we measure the axial field far from the magnet where the field values are low and subject to larger uncertainties. This procedure could produce a large uncertainty in the magnetic moment and the calculated radial magnetic field near the magnet. Consequently, care must be exercised in making these measurements in order to avoid large errors when evaluating the integral contained in Eq. (10). In spite of these difficulties, our final results agree quite well with the measured values of weight and terminal velocity for the magnet.

VII. DISCUSSION

This magnetic braking experiment is an ideal candidate for the undergraduate physics laboratory in electricity and magnetism. Besides being relatively inexpensive, the results are quite dramatic and the principles involved are both fundamental and wide ranging. Our measurements have been presented as a function of the position inside and near the pipe wall. As one might guess, the best results are for values of ϵ and B_r at the center. Thus, for a student run experiment based on a single measurement, the best choice for the depth of the pickup coil or the calculation of B_r would be at the center position. The two approaches represent two levels of computation, one being much less involved than the other. Thus the experiment can be presented at several levels in the physics curriculum.

[1]H. D. Wiederick, N. Gauthier, D. A. Campbell, and P. Rochon, "Magnetic braking: Simple theory and experiment," Am. J. Phys. **55**, 500–503 (1987).

[2]M. A. Heald, "Magnetic braking: Improved theory," Am. J. Phys. **56**, 521–22 (1988).

[3]M. Marcuso, R. Gass, D. Jones, and C. Rowlett, "Magnetic drag in the quasi-static limit: A computational method," Am. J. Phys. **59**, 1118–1123 (1991).

[4]M. Marcuso, R. Gass, D. Jones, and C. Rowlett, "Magnetic drag in the quasi-static limit: Experimental data and analysis," Am. J. Phys. **59**, 1123–1129 (1991).

[5]T. D. Rossing and J. R. Hull, "Magnetic levitation," Phys. Teacher **29**, 552–562 (1991).

[6]W. M. Saslow, "Maxwell's theory of eddy currents in thin conducting sheets, and applications to electromagnetic shielding and MAGLEV," Am. J. Phys. **60**, 693–710 (1992).

[7]The neodymium magnet is available from Arbor Scientific, Ann Arbor, MI.

[8]P. Lorrain and D. R. Corson, *Electromagnetic Fields and Waves*, 2nd ed. (Freeman, San Francisco, 1970) pp. 319–322.

[9]J. R. Merrill, *Using Computers in Physics* (Houghton Mifflin, Atlanta, 1976), pp. 73–88.

SHORT CIRCUITS

When two bulbs are connected in series and a wire is then connected across one of the bulbs (short circuit), many students (even among those in an engineering-physics course) are astonished by the fact that the shorted bulb goes out and the other burns more brightly. They have all heard the term "short circuit" but very few have any operational or conceptual awareness of its meaning, nor do they visualize the accompanying effects. All they know is that a short circuit is something "bad." They should be led into forming the concept through "idea first and name afterwards."

Arnold B. Arons, *A Guide to Introductory Physics Teaching* (Wiley, New York, 1990), p. 171.